

1 **The effect of chemical dispersant concentration on**
2 **hydrocarbon mobility through permeable North-East**
3 **Scotland sands**

4 Luis J. Perez Calderon^{a,b,c}, Lloyd D. Potts^{a,b}, Thomas Cornulier^a, Alejandro Gallego^c, James A.
5 Anderson^b, Ursula Witte^a

6 **Institutional affiliations:**

7 a) Institute of Biological and Environmental Science, University of Aberdeen, Aberdeen,
8 United Kingdom

9 b) Surface Chemistry and Catalysis Group, Materials and Chemical Engineering,
10 Department of Engineering, University of Aberdeen, Aberdeen, United Kingdom

11 c) Marine Scotland Science, Marine Laboratory Aberdeen, Aberdeen, United Kingdom

12 **Corresponding author:** Luis J. Perez Calderon – lj.perezcalderon@gmail.com

13 **Notes:** Colour should be included for Figures 1, 2, 4 and 5.

14 **Author contributions:** LJP, JA and UW conceived the experiment. LJP and LDP collected
15 the samples and carried out the experiment. LJP and TC analysed the data. All authors reviewed
16 the manuscript.

17 **Competing interests:** The authors declare no competing interests.

18 **Potential referees:**

19 • Markus Huettel (Email: mhuettel@fsu.edu; Department of Earth, Ocean and
20 Atmospheric Science, Florida State University, 117 N Woodward Av., Tallahassee,
21 Florida 32306-4320; Website: <http://myweb.fsu.edu/mhuettel/>)

22 • Antje Rusch (Email: rusch@micro.siu.edu; Address: Southern Illinois University,
23 Department of Microbiology, Life Science II 191; Website:
24 <http://micro.siu.edu/faculty-staff/faculty/rusch.php>)

25 • Dongye Zhao (Email: zhaodon@auburn.edu; Address: Department of Civil
26 Engineering, 209 Harbert Engineering Center, Auburn University, AL 36849-5337;
27 Website: <http://www.eng.auburn.edu/users/dzhao/>)

- 28 • Helen K. White (Email: hwhite@haverford.edu; Address: 370 Lancaster Avenue,
29 Haverford, PA 19041; Website: <https://www.haverford.edu/users/hwhite>)

30 **Highlights:**

- 31 • Chemical dispersant increased the mobility of hydrocarbons through permeable sands.
32 • Chemical dispersant enhanced entrainment of oil below manufacturer recommended
33 dosing.
34 • Chemical dispersant selectively entrained hydrocarbons based on their solubility in
35 water.

36 **Abstract:**

37 Accidental releases of oil to the marine environment can reach sensitive shorelines resulting in
38 a wide range of environmental impacts. Chemical dispersant is a response tool employed to
39 minimise damage to coastal ecosystems by facilitating dispersal of oil slicks before they reach
40 shores. However, chemical dispersants may increase entrainment of hydrocarbons into coastal
41 sediments following an oil spill, resulting in higher hydrocarbon residence times in sediments.
42 Here, the effect of dispersant concentration on the entrainment capability of hydrocarbons in
43 permeable coastal sands from North East Scotland (United Kingdom) was evaluated.
44 Hydrocarbon entrainment into sands was facilitated by dispersant application at concentrations
45 below manufacturer-recommended dosage. Percolation of water-soluble hydrocarbons beyond
46 10 cm deep was not affected by chemical dispersant application and water-insoluble
47 component concentrations increased with dispersant concentration. Results highlighted that the
48 application of dispersant readily mobilised less water-soluble hydrocarbons through coastal
49 sands but did not affect pore-water transport of more water-soluble hydrocarbons.

50 **Keywords:** oil, transport, percolation, sediment, dispersant

51 **1 Introduction**

52 Accidental oil releases to the marine environment result in a wide variety of environmental
53 impacts. These are partly determined by the extent to which the oil evaporates, disperses and
54 biodegrades in the water column, settles on the seabed and reaches shores, among other fates
55 (Bandara et al., 2011; Davies and Tibbetts, 1987; Ramseur, 2010). Documented accidents such
56 as the *Deepwater Horizon (DwH)*, *Prestige* and *Exxon Valdez* oil spills resulted in extensive

57 coastal oiling and subsequent environmental impacts which are detectable to this day (Beyer
58 et al., 2016; Levine et al., 2017; Payne et al., 2008).

59 Chemical dispersants were widely used during *DwH* response operations in an attempt to
60 mitigate its environmental impacts, with 5.3 million litres of dispersant applied at the sea
61 surface and 2.9 million litres at the wellhead (~1500 m deep). Dispersant use remains
62 controversial but has been shown to be beneficial under specific circumstances (Prince 2015).
63 The aim of dispersant application is to disperse insoluble and persistent hydrocarbons by
64 dispersing and dissolving oil as small droplets to increase their surface area with the end goal
65 of accelerating physical, chemical and biological oil degradation (Fingas, 2002). Additionally,
66 dispersant was applied at the wellhead during *DwH* to facilitate the removal of volatile
67 hydrocarbons from surfacing oil and reduce the risks of uncontrolled ignition of volatile
68 hydrocarbons on surface waters and inhalation by oil spill responders (International
69 Association of Oil & Gas Producers, 2015). Dispersant increases oil bioavailability by
70 increasing its accessible surface area and enabling microbes to access and utilise oil faster
71 (Hazen et al., 2010). However, by increasing oil bioavailability, dispersant also facilitates the
72 uptake of hydrocarbons by fauna such as filter feeders, marine mammals, seabirds and
73 commercially harvested fish, and can thus result in negative effects for both the marine
74 environment and reach humans through accumulation in the food chain (Beyer et al., 2016).
75 Moreover, dispersants have been found to be toxic to marine organisms and be more persistent
76 than previously thought (White et al., 2012).

77 Dispersed oil, whether mechanically or chemically dispersed, that reaches shorelines can be
78 entrained into sediments where it can persist for decades and act as a reservoir from which
79 contaminants can enter the food chain (Payne et al., 2008). If polyaromatic hydrocarbons
80 (PAHs, hereafter) reach anoxic sediments biodegradation may be limited and consequently
81 higher PAH half-life in sediments could be expected (Widdel et al., 2010). Whilst the mobility
82 of PAHs is especially relevant due to their carcinogenicity and persistence, entrainment of
83 hydrocarbons from other fractions (such as aliphatics and Benzene, Toluene, Ethyl benzene
84 and Xylene, BTEX hereafter) is relevant as these have been shown to induce an environmental
85 response, particularly in microbial communities (Phelps and Young, 1999). BTEX components
86 are far more water-soluble than PAHs, potentially being carried into permeable sediments more
87 readily.

88 Oil contact with sediments is particularly undesirable because of the well-known
89 environmental impacts it causes, the difficulty involved in restoring habitats and the damage
90 to the reputation of the responsible party (Beyer et al., 2016; Zuijggeest and Huettel, 2012).
91 Consequently, understanding the potential entrainment of spilled oil into sediments in coastal
92 environments is relevant. During *DwH*, the shorelines of Louisiana and other southern states
93 of the United States were severely affected by beached oil (Nixon et al., 2016). Zuijggeest and
94 Huettel (2012) assessed the entrainment potential of mechanically and chemically dispersed
95 MC525 oil (using Corexit 9500A) and found that mobility of Total Petroleum Hydrocarbons
96 (TPH, hereafter) and PAHs was increased when a 1:100 Corexit 9500A to oil ratio was applied
97 due to Corexit increasing the solubility of hydrocarbons.

98 Over 70% of the seabed of the North Sea is characterised as fine sand (Paramor et al., 2009).
99 Sandy seabeds are highly permeable and therefore facilitate pore-water flushing. Permeable
100 continental shelf sediments contribute significantly to benthic biogeochemical cycling and
101 primary production (Huettel et al., 2014). This highlights the importance of understanding the
102 capability of hydrocarbons to entrain permeable sediments, which may affect upstream
103 ecological processes should a large-scale oil spill take place.

104 The aims of this work were to evaluate the potential of spilled hydrocarbons to be entrained
105 into permeable sands and the effect of concentration of a commercially available dispersant
106 stockpiled in the United Kingdom (Superdispersant-25, SD25 hereafter) on this process using
107 Schiehallion crude oil and a synthetic oil (model oil, hereafter). A synthetic oil was used as it
108 gives a good intermediate between a single hydrocarbon and a crude oil. Additionally, the use
109 of a synthetic oil enabled a constant mixture that could be replicated and compared between
110 experiments. A further objective was to elucidate if SD25 selectively mobilised components of
111 different fractions of hydrocarbons at increasing SD25 concentration. The hypotheses of this
112 study were: (1) The effects of SD25 on hydrocarbon entrainment into sediments would be
113 observable from below manufacturer recommended application doses, (2) increasing SD25
114 concentration would increase the entrainment of hydrocarbons and would be less effective in
115 facilitating entrainment of the more soluble components of the model oil (such as BTEX and
116 naphthalene) and (3) Oils would readily entrain permeable sands and may do so to different
117 extents due to the difference in composition of the Schiehallion crude and model oils.

118

119 **2 Materials and methods**

120 *2.1 Study site*

121 The present study was conducted using intertidal sandy sediment collected at the mouth of the
122 Ythan estuary (57°18'25.2"N 1°59'13.2"W), which is located 10 km to the north of Aberdeen,
123 North East Scotland (United Kingdom, Figure 1).



124

125 Figure 1. Location of sampling station (purple pin), Ythan estuary, North East Scotland, United
126 Kingdom.

127 The estuary's intertidal area has been estimated at 1.85 km², with a tidal flushing time between
128 <14 hours (Balls, 1994) and 5–12 days (Leach, 1971). The sampling location chosen for this
129 study was at the front-face of the beach. Samples were collected on December 2015 using
130 acrylic cores (internal diameter = 3.6 cm, length = 30 cm) (small cores, hereafter) for sediment
131 analysis and percolation experiments. Further samples were collected using larger cores
132 (internal diameter = 10 cm, length = 30 cm) (large cores, hereafter) to measure permeability.

133 Seawater was collected from the site and UV-filtered (0.5 μm filter). Salient salinity and pH of
134 water used were 35 and 7.5, respectively. The Ythan estuary has been chosen as the study site
135 for this work due to its proximity to oil and gas offshore installations in the North Sea. These
136 sands are representative of Scottish intertidal sands. Moreover, the Ythan Estuary is classified
137 as a Special Protection Area under Article 4.1 of the Birds Directive (79/409/EEC, code:
138 UK9002221, Natura 2000 network), highlighting the importance of understanding the
139 implications of oil beaching in this region.

140 2.2 *Sediment characterisation*

141 All analyses detailed below were conducted on three replicate cores each, which were sectioned
142 into four 2.5 cm sections (i.e. 0–2.5, 2.5–5, 5–7.5 and 7.5–10 cm). Each section was
143 homogenised and subsamples subsequently oven dried at 60°C for three days and mechanically
144 milled to ensure uniform grain size. Total carbon content (TC) was determined using an
145 NA2500 elemental analyser (Carlo Erba Instruments). Total organic carbon content (TOC) was
146 determined by acidification of sediment samples with 10% HCl acid, overnight drying at 60°C
147 and subsequent carbon content quantification. Total inorganic carbon (TIC) content was
148 determined as the difference between TC and TOC.

149 For analysis of grain size distribution, a separate set of subsamples was dried overnight at
150 105°C and subsequently sieved through decreasing mesh sizes (diameter = 2000, 1000, 500,
151 250, 125 and 63 μm). Statistical analyses for the particle size distribution were performed using
152 Gradistat v.8 (Blott and Pye, 2001).

153 Saturated hydraulic conductivity (K_s) was measured using a UMS KSat benchtop saturated
154 hydraulic conductivity instrument using the falling head method (Head, 1982). Three large
155 cores were divided into two sections of depth ranges 0–5 cm, and 5–10 cm. Sectioned sediment
156 samples were saturated with degassed, deionised water prior to recording of the K_s value to
157 ensure no air bubbles were retained within the sediment, which might otherwise distort the
158 measurement. Triplicate measurements were taken for each sample to ensure representative K_s
159 values. Permeability (k) was derived from K_s by the equation:

$$160 \quad k = \frac{K_s m}{\rho g}$$

161 Where ρ and m are the water density (g cm^{-3}) and viscosity ($\text{g cm}^{-1} \text{s}^{-1}$), respectively, and g is
162 gravity (9.81 m s^{-2}).

163 2.3 *Critical Micelle Concentration of Superdispersant-25*

164 The apparent critical micelle concentration (CMC) of SD25 was measured following a similar
165 approach to that used by Gong et al. (2014). Briefly, three stock solutions of SD25 in seawater
166 were prepared ($327 \pm 1 \text{ mg l}^{-1}$) and these were diluted with several volumes of seawater and
167 were measured for surface tension using a tensiometer (Attension, Sigma 700) fitted with a Du
168 Noüy ring (triplicate measurements for each sample). Surface tension was then plotted against
169 \log_{10} SD25 concentration (mg l^{-1}). A value of zero was allocated to $\log_{10}(\text{SD25 concentration}=0)$
170 (mg l^{-1}) for the purposes of establishing the apparent CMC. Thereafter, the change in gradient
171 was used as a boundary to calculate two linear regressions and establish their intersection point
172 which was inferred to be the CMC (Gong et al., 2014).

173 2.4 *Oils used in percolation experiments*

174 A North Sea crude oil (Schiehallion) and a model oil were used in this investigation. The SARA
175 analysis of the Schiehallion crude oil was undertaken externally (Intertek, ITS Testing
176 Services, United Kingdom) and the mass percentage of the four fractions was found to be:
177 saturates 51.33%, aromatics 32.20%, resins 14.87% and asphaltenes 1.5%. C_{10-30} were the most
178 abundant hydrocarbon chain-lengths in the Schiehallion crude oil (Supplementary Figure 1).
179 The model oil was composed of 21 hydrocarbons including BTEX, aliphatic, PAH and resin
180 fractions (Ferguson et al., 2017). The model oil was based on the Schiehallion crude oil to
181 enable a comparison to the crude and analyse the fate of all its components individually. The
182 model oil contained hydrocarbons larger than C_8 because these are more readily deposited on
183 the seabed. Details of the percentage composition by component and fraction can be found in
184 Table 1.

185

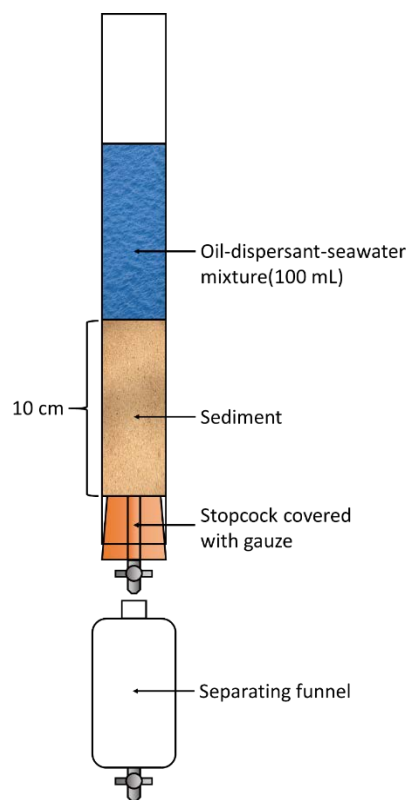
186 Table 1. Synthetic oil composition and selected properties of its components. Octanol-water coefficients
 187 were obtained from literature: (a) Sangster et al. (1989), (b) Mackay et al. (2006), (c) ChemSpider
 188 website, (d) Sigma Aldrich website.

Hydrocarbon	Hydrocarbon class	Molecular weight (g mol ⁻¹)	Octanol-water coefficient (log <i>K_{ow}</i>)	Percentage composition	Sonication extraction efficiency (%)	Liquid-liquid extraction efficiency (%)
Ethyl-Benzene	BTEX (18.0%)	106.165	3.15 ^b	6.1	97.4 ± 0.1	88.5 ± 7.3
m-Xylene		106.165	3.20 ^b	6.0	97.9 ± 0.1	88.7 ± 7.2
o-Xylene		106.165	3.12 ^b	5.9	99.3 ± 0.7	89.5 ± 7.0
Decane	Aliphatics (58%)	142.282	6.25 ^a	9.0	99.1 ± 0.0	89.2 ± 7.0
1-Decene		140.266	4.70 ^b	9.1	98.2 ± 0.6	88.7 ± 7.2
Dodecane		170.334	6.80 ± 1.00 ^a	9.0	99.9 ± 0.0	89.4 ± 7.1
Tetradecane		198.388	8.00 ^a	9.2	100.3 ± 0.1	88.7 ± 6.9
Pentadecane		212.415	7.50 ^b	6.2	101.0 ± 0.2	89.0 ± 7.0
Hexadecane		226.441	8.00 ^b	8.8	101.2 ± 0.2	88.3 ± 6.8
Heptadecane		240.468	8.50 ^b	1.5	101.1 ± 0.0	88.7 ± 7.1
1-Octadecene		252.478	9.81 ^c	1.4	101.2 ± 0.7	88.0 ± 6.9
Eicosane		282.547	10.0 ^b	1.6	101.6 ± 0.5	87.5 ± 7.2
Docosane		310.601	12.44 ^c	1.4	101.8 ± 0.4	88.1 ± 7.0
Tetracosane		338.654	12.0 ^b	1.5	102.4 ± 0.2	87.8 ± 7.8
Naphthalene	PAHs (18.2%)	128.171	3.43 ^b	5.4	99.9 ± 0.7	89.3 ± 6.9
Fluorene		166.219	4.18 ^a	3.1	101.1 ± 0.4	89.3 ± 6.2
Phenanthrene		178.229	4.52 ^a	3.0	100.4 ± 1.3	89.2 ± 6.0
Anthracene		178.229	4.50 ^a	0.7	84.9 ± 4.0	86.9 ± 6.4
Fluoranthene		202.251	5.20 ^a	3.1	101.7 ± 1.0	89.7 ± 6.4
Pyrene		202.201	5.17 ^c	3.0	101.8 ± 1.1	89.6 ± 6.5
Dibenzothiophene	Resin (4.9%)	184.257	4.38 ^a	4.9	101.0 ± 1.7	89.2 ± 6.4

189

190 2.5 Percolation experimental set-up

191 Solutions of SD25 in seawater were prepared by adding SD25 to seawater in one-litre
 192 volumetric flasks. Thereafter, SD25-seawater solutions were magnetically stirred at room
 193 temperature for 24 h to allow equilibration of SD25 in seawater. Immediately before
 194 percolations were performed, 100 ml of each solution was spiked with 1 g of oil and sonicated
 195 (45 kHz) in a USC-TH Ultrasonic bath (VWR) for 3 min to produce a proxy oil in water mixture
 196 to emulate the consequences of mechanical mixing of oil and water by waves and tides. The
 197 percolation experiment was based on a short column experiment by Zuijdgheest & Huettel
 198 (2012) with some modifications (Figure 2).



199

200 Figure 2. Percolation experiment setup.

201 Samples were extruded from the small cores used for collection and transferred to Pyrex cores
 202 of the same dimensions. Care was taken to avoid alteration to the sedimentary structure. The
 203 cores were then fitted with a gauze-lined stopcock to prevent blockage by sand. Sediment in
 204 cores was then saturated with uncontaminated seawater, after which mixtures of oil and SD25
 205 at various concentrations (Table 2) were added to the cores avoiding sediment resuspension.
 206 The highest concentration (333.3 mg l^{-1}) corresponds to the lower boundary of the
 207 manufacturer's recommendations (1:30 dispersant to oil ratio). Immediately after the addition
 208 of the mixtures, the stopcock was opened to allow percolation of the mixtures through the sand
 209 until the water level reached the sediment surface. Washout water was collected and a further
 210 100 ml of non-contaminated water were percolated through the cores using the same method.
 211 The combined washout oil-dispersant-seawater solution was collected in separating funnels
 212 and hydrocarbons were extracted within minutes. Sediment was then extruded and sectioned
 213 by depths (0.0–1.0, 1.0–3.0, 3.0–5.0, 5.0–7.5, 7.5–10.0 cm) for hydrocarbon extraction and
 214 analysis. The use of natural, undisturbed sediments was decided following preliminary
 215 experiments where mixed sand from the upper 10 cm were carried out and showed that mixing
 216 (homogenising) sand resulted in enhanced entrainment and therefore overestimated
 217 entrainment in Ythan estuary sands (Supplementary Figure 2).

218 Table 2. Superdispersant-25 (SD25) concentrations applied to the oils used.

Oil type	SD25 concentration (mg l ⁻¹)					
Control	0	-	-	-	-	-
Schiehallion crude oil	0	-	-	-	-	333.3
Synthetic oil	0	9.8	21.1	42.0	150	333.3

219

220 2.6 Hydrocarbon extraction and analysis

221 Hydrocarbon extractions from sediment were performed by sonicating each sediment section
 222 in 50 ml of dichloromethane for 10 min for model oil-contaminated samples. The procedure
 223 was performed in triplicate for the Schiehallion crude oil-contaminated sediment extractions.
 224 Extractions from washout water were performed by liquid-liquid extraction with 3 × 25 ml
 225 dichloromethane for both oil type-contaminated sediments. Hydrocarbons were quantified
 226 against external standards containing known concentrations of the model oil components.
 227 Hydrocarbon recovery efficiencies for each component can be found in Table 1. Schiehallion
 228 crude oil extractions were subsequently rotary-evaporated at 40°C until all dichloromethane
 229 had evaporated. Model oil extracts were analysed by gas chromatography (GC, hereafter) with
 230 flame ionizing detection using a previously described system (Ferguson et al., 2017). When no
 231 hydrocarbons were detected by GC, extracts were further concentrated by rotary evaporating
 232 to 10 ml and reinjected into the GC. Schiehallion crude oil was analysed gravimetrically as
 233 TPH.

234 Calibration curves (6-point) were determined for each compound of the model oil. Laboratory
 235 control samples were analysed to establish the effect of the sediment matrix and extraction
 236 procedure on the recovery of model oil compounds. Toluene was added (1 µl ml⁻¹) as an
 237 internal standard to correct for injection error in the GC analysis. The limits of detection (LOD)
 238 and quantification (LOQ) were defined as chromatographic signal to noise ratios (S:N) of 3
 239 and 10, respectively. When chromatographic peaks had a S:N between the LOD and LOQ were
 240 assigned a value of LOQ/2.

241 2.7 Chemicals

242 All model oil components (Table 1), toluene (99.8%), dichloromethane (99.8%) and hydrogen
 243 peroxide (30%) were purchased from Sigma Aldrich. SD25 was purchased from Oil Technics
 244 (Aberdeenshire). Sodium hexametaphosphate (technical grade) was purchased from Alfa
 245 Aesar.

246 2.8 Calculations and statistical modelling

247 To establish valid comparisons across SD25 treatments, hydrocarbon concentrations in
248 sediment were normalised to the total mass of hydrocarbon accounted for in all sediment layers
249 and washout as follows:

$$250 \quad C_{i,j,k} = \frac{\frac{m_{i,j,k}}{t_{i,k}}}{s_{j,k}}$$

251 Where $C_{i,j,k}$ is the normalised concentration in sediment of hydrocarbon i in section j in core k ,
252 $m_{i,j,k}$ is the mass of hydrocarbon i in section j in core k , $t_{i,k}$ is the total mass of hydrocarbon i in
253 all sediment layers and washout of core k and $s_{j,k}$ is the mass of sediment in section j in core k .
254 Washout hydrocarbon mass was normalised to total hydrocarbon mass in sediment and
255 washout mixture as follows:

$$256 \quad W_{i,k} = \frac{m_{i,k}}{t_{i,k}}$$

257 Where $W_{i,k}$ is the normalised mass of hydrocarbon i in the washout of core k and $m_{i,k}$ is the
258 mass of hydrocarbon i in the washout mixture of core k . Depth and SD25 were expected to
259 have non-linear effects and interactive effects on C . Therefore, a generalised additive mixed
260 effects model (GAMM) was therefore fitted to the data including, for each individual
261 hydrocarbon, a bivariate tensor product smooth of depth and SD25 (Wood, 2006). Core identity
262 (k) and Hydrocarbon identity (i) were specified as crossed random intercepts which allowed
263 for variation in average C between cores and between model oil components. A lag-1
264 continuous autoregressive residual correlation term was included in the model to account for
265 the lack of independence between depth segments due to the movement of hydrocarbon from
266 the surface of the sediment to the segments underneath, such that C at one depth segment was
267 allowed to depend on C of the same hydrocarbon at the depth segment directly above it. Due
268 to the much higher concentration of hydrocarbons in the 0–1 cm layer compared to the rest of
269 the sediment column ($89.5 \pm 6.8\%$), the data from this layer was omitted from the GAMM. The
270 response variable C was square root transformed prior to fitting the model to improve
271 homoscedasticity of residuals, and a Gaussian distribution was assumed for the data. The model
272 formula was:

$$273 \quad C \sim te(z, SD25, by = i)$$

274 Where C is normalised hydrocarbon concentration, te represents tensor product smooths, z is
275 the sediment depth (cm), $SD25$ is $SD25$ concentration (mg l^{-1}), b_y estimates a separate smoother
276 for each hydrocarbon i . Assessment of W_i as a function of $SD25$ concentration was modelled
277 using locally weighted regression where W_i was the response variable and $SD25$ concentration
278 was the explanatory variable. The model fits a polynomial surface determined by $SD25$
279 concentration as a predictor using local polynomial regression fitting (Cleveland et al., 1992).
280 W_i and $SD25$ concentration were log-scaled for ease of visualisation. For comparisons between
281 Schiehallion and model oil, TPH mass percentages retained at each sediment depth and
282 washout a locally weighed regression was also used where mass percentage was the response
283 variable and depth was the explanatory variable. Models were developed for $SD25$
284 concentration = 0 and 333.3 mg l^{-1} separately, and mass percentage was log-scaled for ease of
285 visualisation. Where pair-wise comparisons were carried out, two-way ANOVAs are used to
286 establish if $SD25$ application and oil type showed significant effects. All statistical analyses
287 were carried out using the statistical software R (R Development Core Team, 2017) and the
288 libraries *ggplot2* (for the locally weighed regression analysis) and *mgcv* (for the GAMM
289 analysis) (Wickham, 2009; Wood, 2011).

290

291 **3 Results**

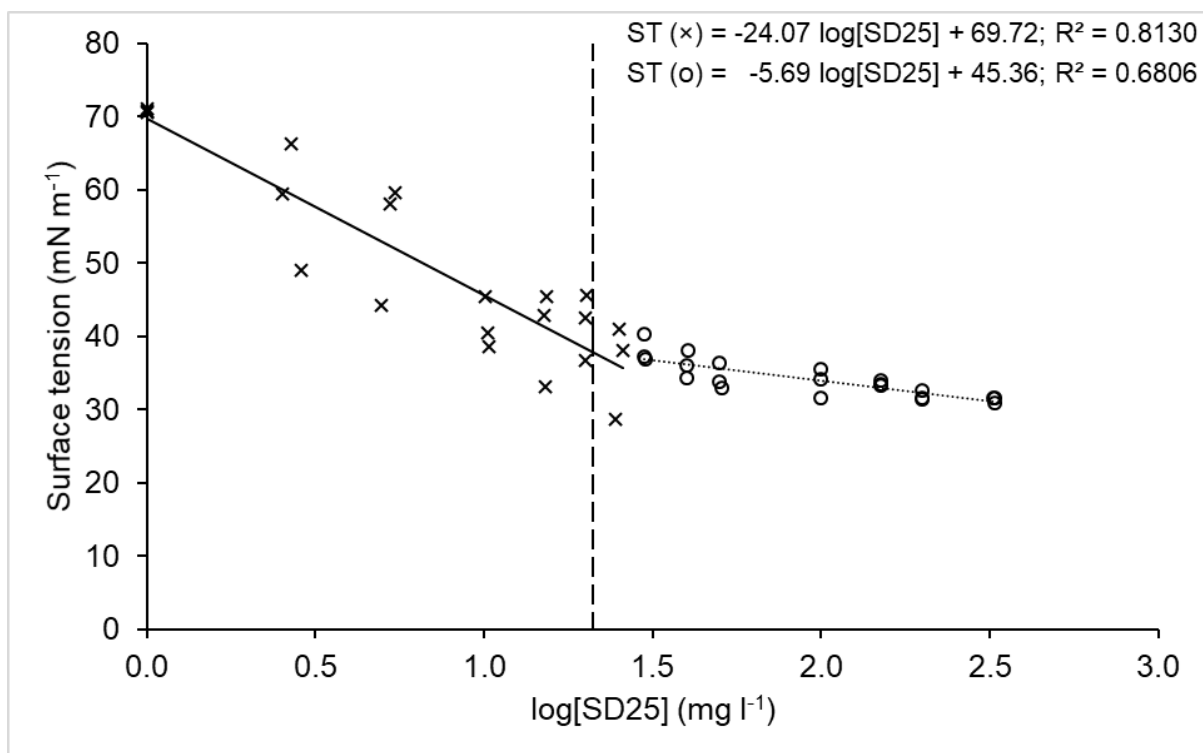
292 *3.1 Sediment properties and SD25 characterisation*

293 The sediments analysed were classified as sands and were found to be highly permeable (Table
 294 3). The intersection of linear response of surface tension to SD25 concentration, the apparent
 295 CMC of SD25 in seawater, as 21.1 mg l⁻¹ (Figure 3).

296 Table 2. Ythan intertidal sediment characteristic. Permeability was measured at larger depth intervals
 297 than the other properties shown due to the size requirement of the instrument used. Errors represent
 298 standard deviation (n = 3). D50, TC, TIC and TOC refer to mass-median-diameter, total carbon, total
 299 inorganic carbon and total organic carbon, respectively.

Sediment size and sorting			Carbon content			Permeability	
Depth (cm)	D ₅₀ (µm)	Sorting	TC (%)	TIC (%)	TOC (%)	Depth (cm)	Permeability (m ²)
0.0–2.5	299.1 ±	Moderately Well	0.072 ±	0.043 ±	0.029 ±	0.0–5.0	4.04 × 10 ⁻¹¹ ± 2.25 × 10 ⁻¹²
	11.4	Sorted Medium Sand	0.024	0.028	0.006		
2.5–5.0	309.8 ±	Moderately Well	0.052 ±	0.038 ±	0.014 ±		
	6.6	Sorted Medium Sand	0.045	0.033	0.012		
5.0–7.5	334.5 ±	Moderately Well	0.086 ±	0.061 ±	0.026 ±	5.0–10	4.54 × 10 ⁻¹¹ ± 4.99 × 10 ⁻¹²
	20.3	Sorted Medium Sand	0.012	0.018	0.006		
7.5–10	328.7 ±	Slightly Very Fine	0.038 ±	0.019 ±	0.019 ±		
	5.3	Gravelly Medium Sand	0.010	0.008	0.005		

300

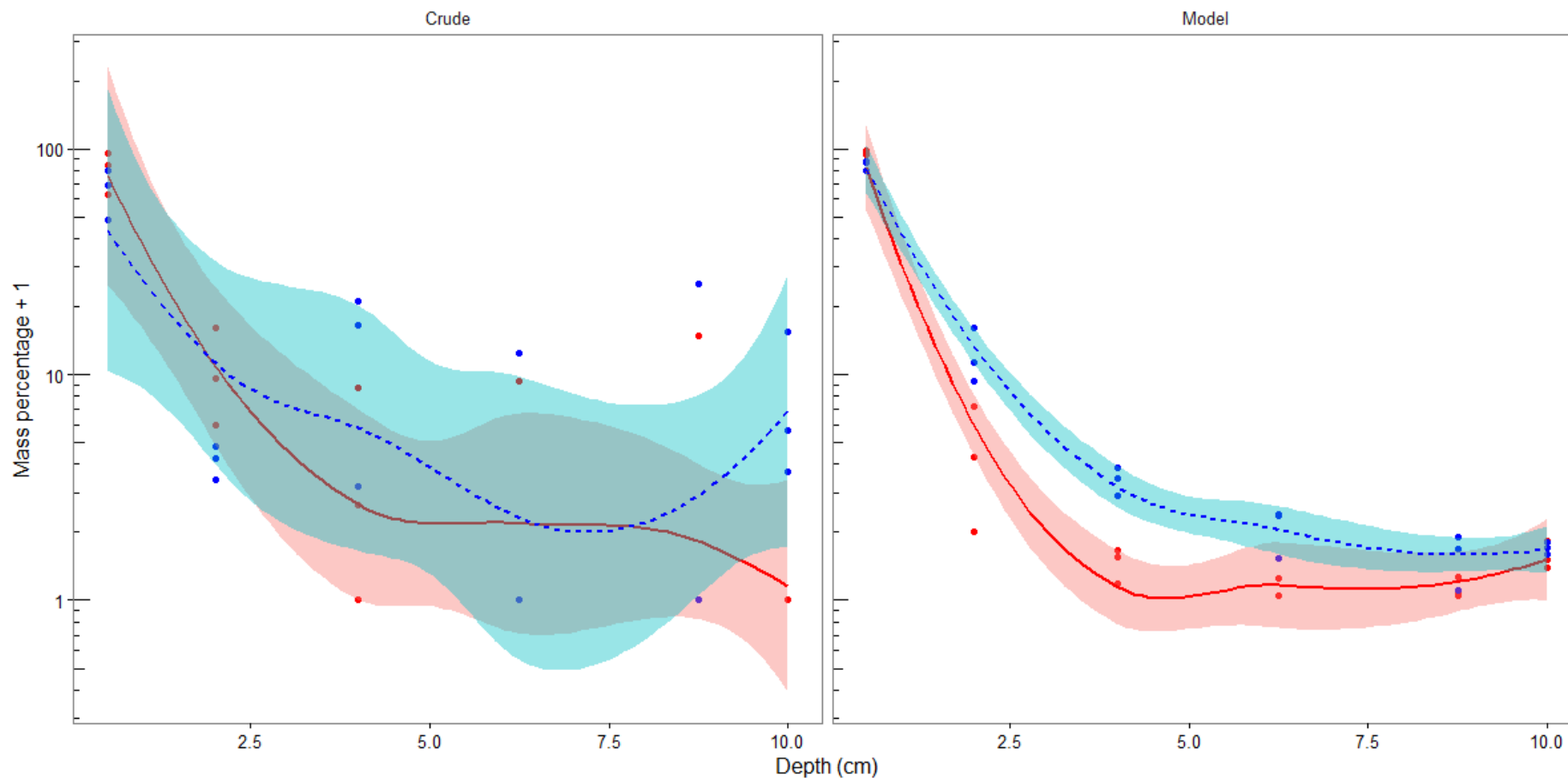


301

302 Figure 3. Surface tension of Ythan seawater as a function of Superdispersant-25 (SD25) concentration
 303 to establish the apparent critical micelle concentration of SD25. Crosses and circles denote the
 304 separation of the dataset to calculate linear regressions (solid and dotted lines, respectively) from the
 305 change of slope and their intersection (vertical dashed line).

306 3.2 Model oil – Schiehallion crude oil comparison

307 The proportion of TPH retained in the top layer (0–1 cm) for model oil was significantly higher
 308 than that of Schiehallion crude oil aggregating treatments of both oil, and oil and dispersant
 309 treatments ($89.5 \pm 6.8\%$ and $72.4 \pm 16.9\%$, respectively, p -value = 0.04). Dispersant
 310 recommended dosage reduced the percentage to TPH retained in the top layer for model oil
 311 ($95.1 \pm 2.4\%$ to $83.9 \pm 4.1\%$, $p = 0.01$) but not for crude oil ($79.9 \pm 17.0\%$ to $64.9 \pm 16.1\%$, p
 312 = 0.33). Mass percentage decreased exponentially with depth for both oils and treatments.
 313 Locally weighed regressions revealed a clear increase in mass percentage as depth increased
 314 for model oil but not for crude oil when SD25 was applied at recommended dosage (Figure 4)
 315 SD25 did not have a consistent effect on the mass percentage of Schiehallion crude oil retained
 316 at any sediment layer but did increase the percentage of oil in the washout ($3.7 \pm 5.7\%$ and 0%
 317 when SD25 was not applied).

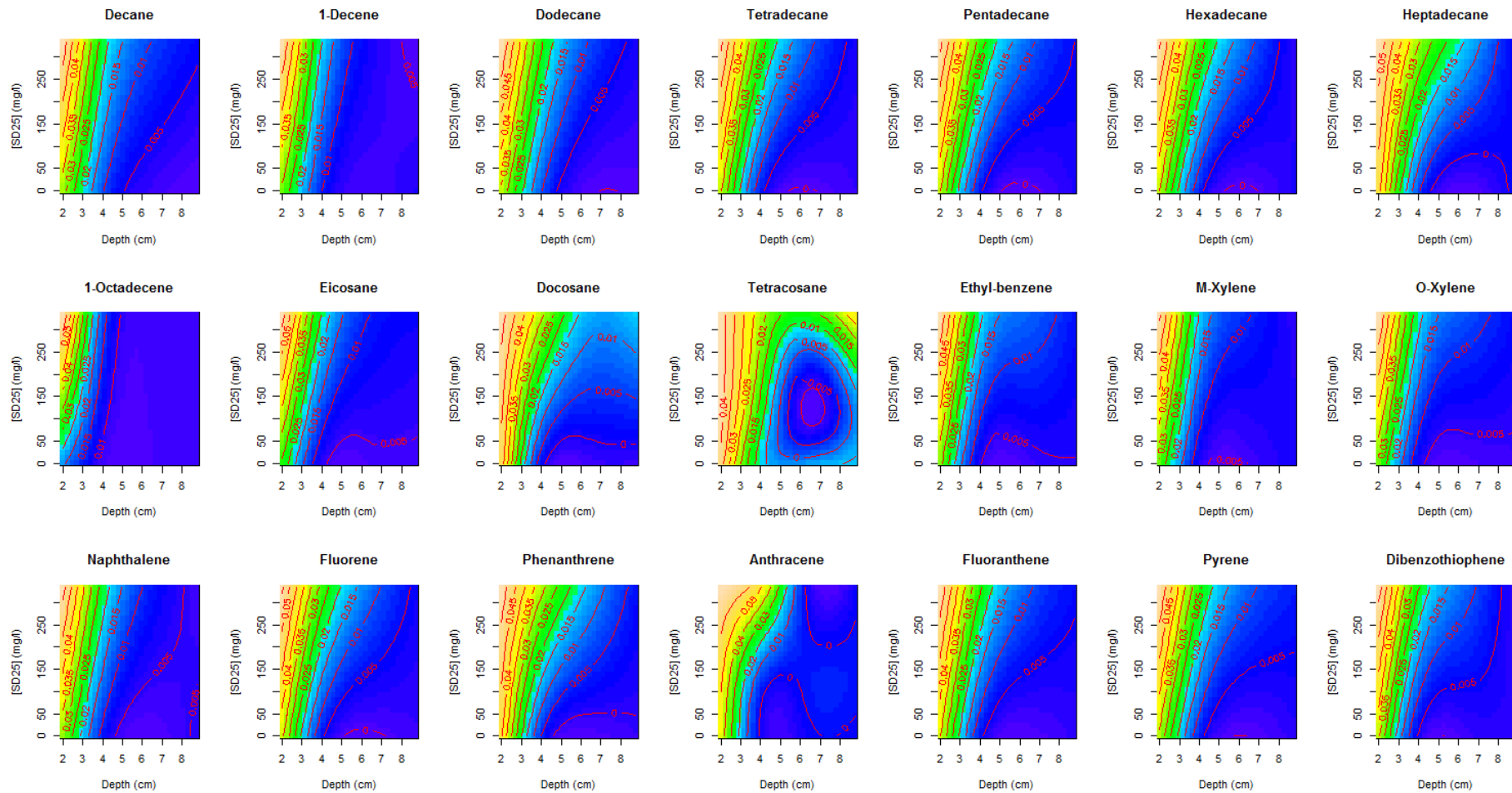


318

319 Figure 4. Total hydrocarbon mass percentage as a function of depth by treatment. Oils used were crude oil (left) and model oil (right) and treatments were oil
 320 only (red dots) and oil and 333.3 mg l⁻¹ Superdispersant-25 (blue dots). Oil (red) and Oil and dispersant (blue) treatment lines bands represent locally-weighted
 321 regression values and associated standard errors, respectively. Note mass percentage has been log(x+1)-scaled.

322 3.3 *Hydrocarbon entrainment into the top 10 cm of sediment*

323 The GAMM results indicate that the application of SD25 increased the normalised
324 concentration of all hydrocarbons with depth, even at SD25 concentration below the
325 recommended dosing (Figure 5, Supplementary Figure 3, Supplementary Table 1). Overall, the
326 application of SD25 increased the amount of oil entrained into these sands. The effect of SD25
327 was similar for most hydrocarbons in the top 4 cm. However, differences in the effect of SD25
328 on the entrainment of hydrocarbons became apparent at depths greater than 4 cm. C₁₀₋₁₂
329 aliphatics showed a linear increase in entrainment with increasing SD25 concentration as in
330 the surface layers. The remaining hydrocarbons showed increased entrainment into these sands
331 at SD25 concentration above 42 mg l⁻¹. 1-Octadecene showed an unexpected response
332 compared to equivalent length aliphatics (C₁₇ and C₁₉) with no effect of SD25 concentration
333 on entrainment over 5 cm deep. Dibenzothiophene, the only resin in the model oil, showed
334 enhanced entrainment in sediments from low SD25 concentration. Interestingly, entrainment
335 of dibenzothiophene did not increase with dispersant concentration in the range 150–333 mg
336 SD25 l⁻¹ at depths greater than 7 cm.

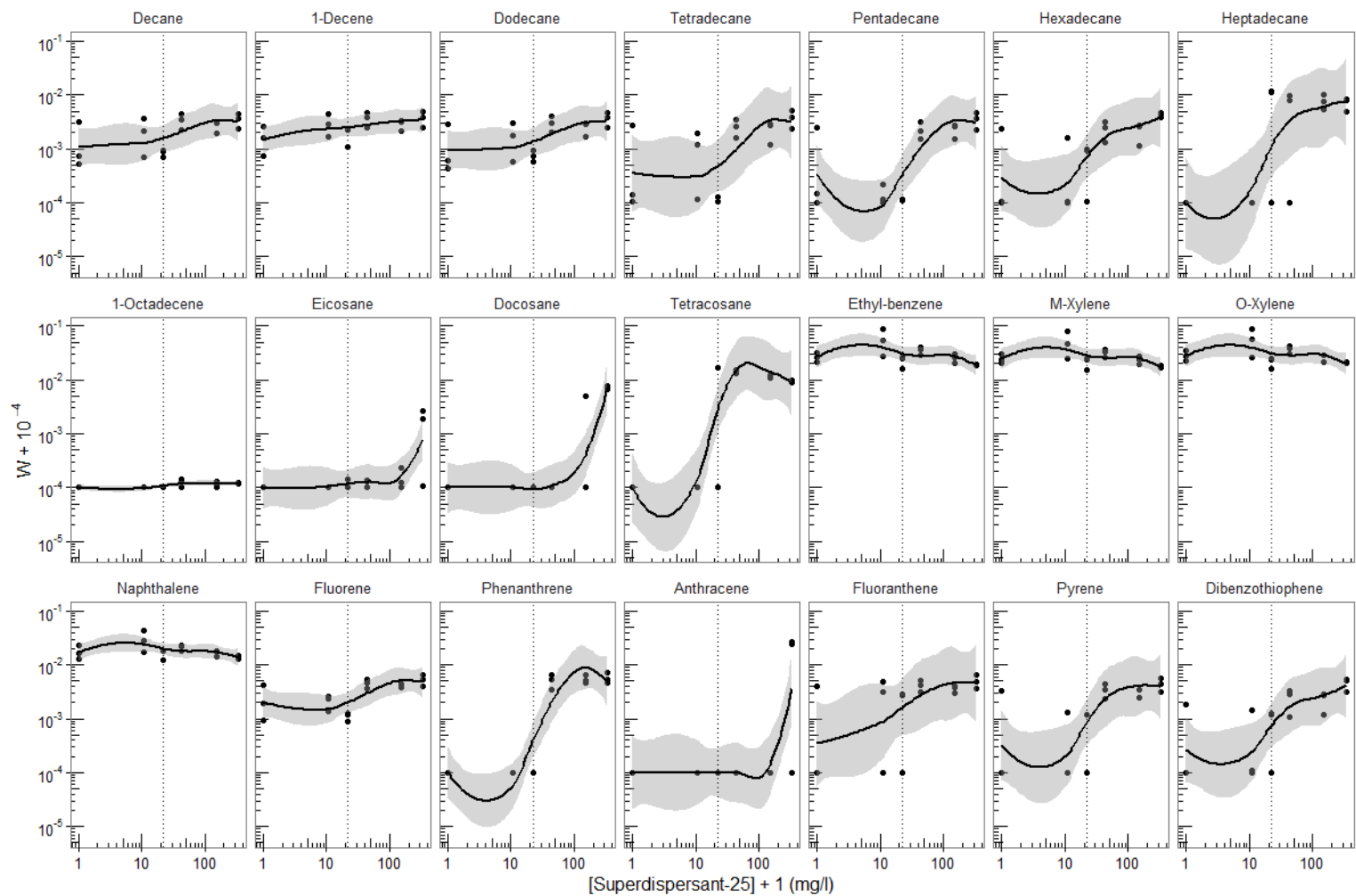


337

338 Figure 4. Generalised additive mixed effects models of hydrocarbon concentration in Ythan intertidal sands following percolation with increasing
 339 Superdispersant-25 concentrations from sediment depths of 1 to 10 cm. Note hydrocarbon concentrations have been normalised and square-rooted.

340 3.4 Hydrocarbon entrainment beyond 10 cm of sediment

341 W_i in the washout varied by component and SD25 concentration (Figure 6). For C_{10-14}
342 aliphatics, the influence of SD25 concentration on W_i was unclear. $W_{\text{Pentadecane}}$ (C_{15}) was
343 increased at 42 mg SD25 l^{-1} but higher concentrations did not result in further increases of
344 $W_{\text{Pentadecane}}$. $W_{\text{Hexadecane}}$ (C_{16}) increased with SD25 concentration. Heptadecane (C_{17}) and
345 tetracosane (C_{24}) showed a higher W_i at and above 21.1 mg SD25 l^{-1} . Interestingly, SD25
346 application did not affect $W_{1\text{-Octadecene}}$ (C_{18}) but affected C_{20} and C_{22} aliphatics which only
347 increased at SD25 concentration >150 mg l^{-1} . For the more soluble components of the model
348 oil such as BTEX and naphthalene, no clear effect of SD25 concentration was observed, with
349 W_i fluctuating as SD25 concentration increased. The response of fluorene to SD25
350 concentration was similar to that of C_{10-15} aliphatics, but with only a slight increase of W_{Fluorene}
351 at SD25 concentration above 21.1 mg l^{-1} . Larger PAHs showed increased W_i from 42 mg SD25
352 l^{-1} except anthracene which only showed increased $W_{\text{Anthracene}}$ at 333.3 mg SD25 l^{-1} , possibly
353 as a result of its lower percentage composition of the model oil. Dibenzothiophene, showed a
354 steady increase in $W_{\text{Dibenzthiophene}}$ with SD25 concentration.



355

356 Figure 5. Normalised hydrocarbon mass in washout mixtures (W) as a function of Superdispersant-25 concentration. Points represent raw data and lines with
 357 grey bands represent locally-weighted regression values and associated standard errors, respectively. Note W and Superdispersant-25 concentration were
 358 $\log(x+10^{-4})$ and $\log(x+1)$ -scaled, respectively.

359 4 Discussion

360 4.1 Key findings

361 SD25 application enhanced the mobility of hydrocarbons of the model oil through the top 10
362 cm of sediment and increased the W_i of leached hydrocarbons. The effect was most pronounced
363 at and above 150 mg l⁻¹ (half of the recommended dosage in terms of SD25:oil ratio) (Figures
364 5 and 6). The effect of SD25 application on W_i varied with hydrocarbon type, with BTEX and
365 naphthalene being unaffected and the remaining components showing different degrees of
366 response (Figure 6). Overall, the recommended dosing of SD25 (1:30 SD25:oil ratio, 333.3 mg
367 SD25 l⁻¹) increased the W_i of most hydrocarbons. Crude and model oil concentrations followed
368 an exponentially decaying trend with depth in the percentage of mass of TPHs retained in the
369 sediment. SD25 application resulted in increased mobility of model oil through sediments but
370 not in the relative amount of oil in the washout. In contrast, SD25 application resulted in an
371 increase (from zero) in the percentage of crude oil present in the washout.

372 4.2 Sediment properties and Superdispersant-25 CMC

373 The sands used in this experiment were highly permeable (4×10^{-11} m², Table 3) and values
374 were in agreement with prior characterisation of the estuary's sands (Zetsche et al., 2011). High
375 permeability in the top 10 cm results in advective pore-water fluxes being the dominant
376 transport mechanism of solutes (Huettel et al., 2014). Consequently, oil deposition on these
377 permeable sands may result in significant hydrocarbon entrainment after an oil spill. This was
378 evidenced here, where oil entrained the permeable sands beyond 10 cm deep (Figure 6) and is
379 undesirable because sediment-entrained oil can persist for years (Lindeberg et al., 2017).

380 The apparent CMC of SD25 was calculated to be 21.1 mg l⁻¹ (Figure 3), which is close to that
381 reported for Corexit EC9500A (22.5 mg l⁻¹), a dispersant widely used during *DwH* (Gong et
382 al. 2014), suggesting that the surfactant effect of the dispersants may be similar. The relevance
383 of the CMC has been subject to extensive study within remediation and oil spill science in
384 recent years. The desired effects of dispersant are frequently found above the CMC (Ahn et al.,
385 2010; Gong et al., 2014; Zhao et al., 2015). Here, a similar response for SD25 was found for
386 heptadecane and tetracosane leading to increased percolation over 10 cm at SD25 concentration
387 = CMC (Figure 6). It has been shown that different commercial dispersants can have different
388 effectiveness on spilt oil deposition. For example, Corexit dispersants accelerate settling of oil-
389 mineral aggregates more effectively than SPC1000 (Cai et al., 2017). Furthermore, Corexit

390 dispersants promote photodegradation whereas SPC1000 inhibits it (Fu et al., 2016). It is
391 therefore important to establish the effects of dispersants such as SD25, which are stored to
392 respond to potential oil spills across the world, to adequately assess the implications of their
393 use and subsequent consequences.

394 *4.3 Model oil – Crude oil comparison*

395 SD25 application resulted in increased mobility of model oil components but the effect on
396 Schiehallion crude oil was less consistent (Figure 4) This may have been due to the greater
397 complexity of crude oil composition (1000s of components) compared to that of the model oil
398 (21 components), which showed a distinct exponentially decreasing percentage retained at
399 increasing sediment depth. Additionally, the method used to establish TPHs for the
400 Schiehallion crude oil may be less robust than that used for the model oil (gravimetry vs. gas
401 chromatography, respectively). However, the use of a simpler oil (i.e. a model oil) facilitated
402 the interpretation of oil-dispersant interaction mechanisms in seawater and highlighted the need
403 for further research to understand the behaviour of multi-component mixtures in a multi-media
404 system such as the oil-dispersant-seawater-sediment system analysed in this work.

405 *4.4 Hydrocarbon entrainment into the top 10 cm of sand*

406 SD25 application had distinct effects on the mobility of hydrocarbons through permeable sands
407 (Figure 5). SD25 concentration below 42 mg SD25 l⁻¹ had a relatively low impact on the
408 mobility of most hydrocarbons in the top 10 cm. The effect was most apparent at high SD25
409 concentration, indicating that SD25 concentration >150 mg l⁻¹ may be necessary for
410 hydrocarbons to readily entrain into these sands. C₁₀₋₁₂ entrainment showed a linear increase
411 with SD25 concentration (Figure 5). These components are of limited concern as they are
412 relatively volatile and are readily biodegraded (Liu and Liu, 2013). Longer-chained aliphatics
413 (C₁₂₊) responded non-linearly but almost always monotonically to an increase in SD25
414 concentration (Figure 5). C₁₄₋₁₆ were readily mobilised around 4 cm deep at the recommended
415 SD25 dosing compared to in its absence. This suggested that SD25 selectively mobilised
416 aliphatics with long chains more readily than those with short ones. Interestingly, the effect of
417 SD25 application on 1-octadecene entrainment was minimal compared to the C₁₇ and C₂₀
418 saturate hydrocarbons of the model oil (Figure 5). A key difference which may influence 1-
419 octadecene's interactions with an oil-dispersant-seawater-sediment system with respect to C₁₇
420 and C₂₀ saturate hydrocarbons is the presence of a double bond, promoting stronger adsorption
421 to sediment surfaces than saturates. Analogue comparisons between decane (C₁₀ paraffin) and

422 1-decene (C_{10} olefin) reveal that entrainment of 1-decene is less pronounced than that of decane
423 in the top 4 cm of sediment but not deeper (Figure 5). This suggested that SD25 may be less
424 effective in mobilising olefins compared to paraffin. BTEX components showed a limited
425 increase in entrainment with SD25 concentration up to 150 mg l^{-1} , which agrees with previous
426 work on the limited effect of SD25 on the dissolution and dispersion of these components of
427 the model oil in seawater (Perez Calderon et al., 2018). These components were found in higher
428 (normalised) concentrations in the washout hydrocarbon-dispersant-water solution (Figure 6),
429 highlighting the capability of hydrocarbons to be entrained into coastal permeable sediments
430 beyond 10 cm and impact benthic ecosystems. SD25 recommended dosing (1:30 SD25:oil
431 ratio, in this work 333.3 mg l^{-1}) resulted in enhanced entrainment of BTEX components (Figure
432 5). However, unless an oil spill occurs nearshore, it is unlikely that these hydrocarbons will
433 reach coastal sediments due their high volatility and low K_{OW} . Nevertheless, BTEX have been
434 detected in coastal sediment (Phelps and Young, 1999) and consequently, following the
435 precautionary principle, these interactions should be considered in any dispersant application
436 decision-making process. Dispersant-facilitated adsorption has been shown for PAHs using the
437 dispersant Corexit 9500 (Gong et al., 2014; Zhao et al., 2015). In this work, PAHs showed a
438 similar response to C_{14+} aliphatics with an increase in hydrocarbon entrainment with SD25
439 concentration in the top 4 cm of sediment and the effect becoming more pronounced over 4 cm
440 deep. Dispersant application is typically carried out offshore where high-energy mixing can
441 take place with the aim of preventing beaching of spilled oil. However, dispersant can enhance
442 the entrainment into permeable sands by increasing the solubility of hydrocarbons and reducing
443 droplet size.

444 *4.5 Hydrocarbon entrainment beyond 10 cm of sediment*

445 Washout of hydrocarbons over 10 cm deep in Ythan estuary sands was enhanced by SD25
446 application for most hydrocarbons (Figure 6). Aliphatic hydrocarbons of specific chain length
447 ranges (C_{15-17} and C_{20-24}) increased their W_i with SD25 application. In contrast, the effect of
448 SD25 was less apparent on C_{10-14} and C_{18} aliphatics suggesting that SD25 may selectively
449 enhance the mobility of certain hydrocarbons in permeable sediments. C_{10-14} aliphatics are the
450 most soluble alkanes of the model oil and, therefore, a lesser impact of SD25 was expected.
451 Intertidal microbial communities play an important role in organic carbon processing in marine
452 sediments (Woulds et al., 2016). Facilitated entrainment of these hydrocarbons may result in
453 microbial community succession in intertidal permeable sands shifting the microbial
454 composition to hydrocarbon degrading communities (Lamendella et al., 2014). Furthermore,

455 bacterial oxidation of hydrocarbons may increase their water-solubility, making them more
456 mobile within the sediment. The W_i of the most water-soluble hydrocarbons of the model oil
457 (BTEX components and naphthalene) varied across the SD25 concentration range analysed
458 and SD25 application did not have a consistent effect on the capacity of these hydrocarbons to
459 entrain sands beyond 10 cm deep. This is may be due to their high water-solubilities which
460 may limit the effect of SD25 application (Perez Calderon et al., 2018). Previous work has
461 shown a reduced effect of dispersant application on the solubilisation of naphthalene, compared
462 to pyrene (Zhao et al., 2015). This suggests that SD25 enhances the mobility of BTEX
463 components and naphthalene into permeable sands but not their dissolution or dispersion in
464 seawater, implying that pore-water transport of dissolved BTEX and naphthalene is less
465 affected by dispersant application than that of larger, less seawater-soluble hydrocarbons.
466 Larger PAHs (>2 rings) showed a similar response with low W_i values below 42 mg SD25 l⁻¹.
467 However, there was an inflexion point between the CMC and 42 mg SD25 l⁻¹ from which
468 hydrocarbon entrainment increases for these PAHs, indicating that a threshold in enhancing
469 solubility in water may exist for SD25 effectiveness on large PAHs. Dibenzothiophene showed
470 a steady increase in W_i with SD25 concentration, indicating a different response to SD25 than
471 the other PAHs. Dibenzothiophene was the only resin (contains sulphur in its structure) in the
472 model oil, which may explain its higher W_i at low SD25 concentration. Overall, these results
473 suggested that hydrocarbons within a mixture such as a crude oil entrain permeable sediments
474 and solubilise to different extents and that dispersant application affected this process
475 differently for specific groups of hydrocarbons.

476 **5 Conclusions**

477 This work highlighted the capability of a synthetic hydrocarbon mixture (model oil) and a crude
478 oil (Schiehallion) to entrain permeable sands *via* natural percolation and the facilitation of this
479 process by dispersant application. The main findings of the work were:

- 480 (1) A positive effect of SD25 concentration on hydrocarbon mobility was observed below
481 the manufacturer's recommended dosing in permeable sands. Enhanced percolation
482 beyond 10 cm deep was detectable at as low as SD25 CMC (21.1 mg l⁻¹).
- 483 (2) SD25 concentration increased the mobility of model oil through permeable sands and
484 selectively mobilised larger hydrocarbon components (less water-soluble) than smaller
485 components (more water-soluble) of the model oil.

486 (3) Both the model and Schiehallion crude oils readily entrained permeable North East
487 Scotland sands. The concentration profiles by depth followed an exponential decay
488 pattern for model oil but were poorly reproduced for crude oil, highlighting the
489 complexity of interactions in crude oil mobility through permeable media. SD25
490 application increased the entrainment of model oil but not of Schiehallion crude oil,
491 again due to high variability.

492 The findings of this work highlight the potential of oil to readily be entrained into permeable
493 sands in the event of an oil spill and that dispersant application exacerbates the process for
494 some oil components more than others. Further work is needed to understand how different
495 commercial dispersant formulations can affect oil entrainment and how this varies by oil,
496 hydrocarbon and sediment type as well as how seawater moves through sandy sediments and
497 potentially displaces hydrocarbons already present in them.

498 **6 Acknowledgements**

499 The authors acknowledge Paul Hallett and Annette Raffan for granting access to and training
500 on the tensiometer, respectively. Cruickshank Analytical Lab staff are acknowledged for
501 assistance in carbon content analysis. MarCRF is acknowledged for funding LJP's PhD project.
502 BP are acknowledged for providing Schiehallion crude oil.

503 **7 References**

504 Ahn, C.K., Woo, S.H., Park, J.M., 2010. Selective adsorption of phenanthrene in nonionic–
505 anionic surfactant mixtures using activated carbon. *Chem. Eng. J.* 158, 115–119.
506 <https://doi.org/10.1016/j.cej.2009.12.014>

507 Balls, P.W., 1994. Nutrient Inputs to Estuaries from Nine Scottish East Coast Rivers; Influence
508 of Estuarine Processes on Inputs to the North Sea. *Estuar. Coast. Shelf Sci.* 39, 329–352.
509 <https://doi.org/10.1006/ecss.1994.1068>

510 Bandara, U.C., Yapa, P.D., Xie, H., 2011. Fate and transport of oil in sediment laden marine
511 waters. *J. Hydro-environment Res.* 5, 145–156. <https://doi.org/10.1016/j.jher.2011.03.002>

512 Beyer, J., Trannum, H.C., Bakke, T., Hodson, P. V., Collier, T.K., 2016. Environmental effects
513 of the Deepwater Horizon oil spill: A review. *Mar. Pollut. Bull.* 110, 28–51.
514 <https://doi.org/10.1016/j.marpolbul.2016.06.027>

515 Blott, S.J., Pye, K., 2001. GRADISTAT: a Grain Size Distribution and Statistics Package for
516 the Analysis of Unconsolidated Sediments. *Earth Surf. Process. Landforms* 26, 1237–
517 1248. <https://doi.org/10.1002/esp.261>

518 Cai, Z., Fu, J., Liu, W., Fu, K., O'Reilly, S.E.E., Zhao, D., 2017. Effects of oil dispersants on
519 settling of marine sediment particles and particle-facilitated distribution and transport of
520 oil components. *Mar. Pollut. Bull.* 114, 408–418.
521 <https://doi.org/10.1016/j.marpolbul.2016.09.057>

522 Cleveland, W.S., Grosse, E., Shyu, W.M., 1992. Local regression models, in: Chambers, J.M.,
523 Hastie, T.J. (Eds.), *Statistical Models in S*. Wadsworth & Brooks/Cole.

524 Davies, J.M., Tibbetts, P.J.C., 1987. The use of in situ benthic chambers to study the fate of oil
525 in sublittoral sediments. *Estuar. Coast. Shelf Sci.* 24, 205–223.
526 [https://doi.org/10.1016/0272-7714\(87\)90065-5](https://doi.org/10.1016/0272-7714(87)90065-5)

527 Ferguson, R.M.W., Gontikaki, E., Anderson, J.A., Witte, U., 2017. The Variable Influence of
528 Dispersant on Degradation of Oil Hydrocarbons in Subarctic Deep-Sea Sediments at Low
529 Temperatures (0–5 °C). *Sci. Rep.* 7, 2253. <https://doi.org/10.1038/s41598-017-02475-9>

530 Fingas, M.F., 2002. A review of literature related to oil spill dispersants especially relevant to
531 Alaska. Prince William Sound Reg. citizens Advis. Counc. Anchorage, Alaska.

532 Fu, J., Gong, Y., Cai, Z., O'Reilly, S.E., Zhao, D., 2016. Mechanistic investigation into
533 sunlight-facilitated photodegradation of pyrene in seawater with oil dispersants. *Mar.*
534 *Pollut. Bull.* 114, 751–758. <https://doi.org/10.1016/j.marpolbul.2016.10.077>

535 Gong, Y., Zhao, X., O'Reilly, S.E., Qian, T., Zhao, D., 2014. Effects of oil dispersant and oil
536 on sorption and desorption of phenanthrene with Gulf Coast marine sediments. *Environ.*
537 *Pollut.* 185, 240–249. <https://doi.org/10.1016/j.envpol.2013.10.031>

538 Hazen, T.C., Dubinsky, E. a, DeSantis, T.Z., Andersen, G.L., Piceno, Y.M., Singh, N., Jansson,
539 J.K., Probst, A., Borglin, S.E., Fortney, J.L., Stringfellow, W.T., Bill, M., Conrad, M.E.,
540 Tom, L.M., Chavarria, K.L., Alusi, T.R., Lamendella, R., Joyner, D.C., Spier, C., Baelum,
541 J., Auer, M., Zemla, M.L., Chakraborty, R., Sonnenthal, E.L., D'haeseleer, P., Holman,
542 H.-Y.N., Osman, S., Lu, Z., Van Nostrand, J.D., Deng, Y., Zhou, J., Mason, O.U., 2010.
543 Deep-Sea Oil Plume Enriches Indigenous Oil-Degrading Bacteria. *Science* (80-.). 330,
544 204–208. <https://doi.org/10.1126/science.1195979>

545 Head, H.K., 1982. Manual of soil laboratory testing, Vol 2. Pentech Press.

546 Huettel, M., Berg, P., Kostka, J.E., 2014. Benthic Exchange and Biogeochemical Cycling in
547 Permeable Sediments. *Ann. Rev. Mar. Sci.* 6, 23–51. [https://doi.org/10.1146/annurev-](https://doi.org/10.1146/annurev-marine-051413-012706)
548 [marine-051413-012706](https://doi.org/10.1146/annurev-marine-051413-012706)

549 International Association of Oil & Gas Producers, 2015. Dispersants : subsea application Good
550 practice guidelines for incident management and emergency response personnel.

551 Lamendella, R., Strutt, S., Borglin, S., Chakraborty, R., Tas, N., Mason, O.U., Hultman, J.,
552 Prestat, E., Hazen, T.C., Jansson, J.K., 2014. Assessment of the Deepwater Horizon oil
553 spill impact on Gulf coast microbial communities. *Front. Microbiol.* 5, 130.
554 <https://doi.org/10.3389/fmicb.2014.00130>

555 Leach, J.H., 1971. Hydrology of the Ythan Estuary With Reference to Distribution of Major
556 Nutrients and Detritus. *J. Mar. Biol. Assoc. United Kingdom* 51, 137.
557 <https://doi.org/10.1017/S0025315400006536>

558 Levine, B.M., White, J.R., DeLaune, R.D., 2017. Impacts of the long-term presence of buried
559 crude oil on salt marsh soil denitrification in Barataria Bay, Louisiana. *Ecol. Eng.* 99,
560 454–461. <https://doi.org/10.1016/j.ecoleng.2016.11.017>

561 Lindeberg, M.R., Maselko, J., Heintz, R.A., Fugate, C.J., Holland, L., 2017. Conditions of
562 persistent oil on beaches in Prince William Sound 26 years after the Exxon Valdez spill.
563 *Deep Sea Res. Part II Top. Stud. Oceanogr.* <https://doi.org/10.1016/j.dsr2.2017.07.011>

564 Liu, Z., Liu, J., 2013. Evaluating bacterial community structures in oil collected from the sea
565 surface and sediment in the northern Gulf of Mexico after the Deepwater Horizon oil spill.
566 *Microbiologyopen* 2, 492–504. <https://doi.org/10.1002/mbo3.89>

567 Nixon, Z., Zengel, S., Baker, M., Steinhoff, M., Fricano, G., Rouhani, S., Michel, J., 2016.
568 Shoreline oiling from the Deepwater Horizon oil spill. *Mar. Pollut. Bull.* 107, 170–178.
569 <https://doi.org/10.1016/j.marpolbul.2016.04.003>

570 Paramor, O.A.L., Allen, K.A., Aanesen, M., Armstrong, C., Hegland, T., Le Quesne, W.,
571 Raakaer, G.J., Roger, S., van Hal, R., van Hoof, L.J.W., van Overzee, H.M.J., Frid, C.L.J.,
572 2009. MEFEPO North Sea Atlas, University of Liverpool.

573 Payne, J.R., Driskell, W.B., Short, J.W., Larsen, M.L., 2008. Long term monitoring for oil in
574 the Exxon Valdez spill region. *Mar. Pollut. Bull.* 56, 2067–2081.

575 <https://doi.org/10.1016/j.marpolbul.2008.07.014>

576 Perez Calderon, L. J., Potts, L. D., Gontikaki, E., Gubry-Rangin, C., Cornulier, T., Gallego, A.,
577 Anderson, J., Witte, U. (2018). Bacterial Community Response in Deep Faroe-Shetland
578 Channel Sediments Following Hydrocarbon Entrainment With and Without Dispersant
579 Addition. *Frontiers in Marine Science*, 5. <https://doi.org/10.3389/fmars.2018.00159>

580 Phelps, C.D., Young, L.Y., 1999. Anaerobic biodegradation of BTEX and gasoline in various
581 aquatic sediments. *Biodegradation* 10, 15–25. <https://doi.org/10.1023/A:1008303729431>

582 Prince, R.C., 2015. Oil spill dispersants: Boon or bane? *Environ. Sci. Technol.* 49, 6376–6384.
583 <https://doi.org/10.1021/acs.est.5b00961>

584 R Development Core Team, 2017. R: A language and environment for Statistical computing.
585 R Found. Stat. Comput.

586 Ramseur, J., 2010. Deepwater Horizon oil spill: the fate of the oil.

587 White, H.K., Hsing, P.-Y., Cho, W., Shank, T.M., Cordes, E.E., Quattrini, A.M., Nelson, R.K.,
588 Camilli, R., Demopoulos, A.W.J., German, C.R., Brooks, J.M., Roberts, H.H., Shedd, W.,
589 Reddy, C.M., Fisher, C.R., 2012. Impact of the Deepwater Horizon oil spill on a deep-
590 water coral community in the Gulf of Mexico. *Proc. Natl. Acad. Sci.* 109, 20303–20308.
591 <https://doi.org/10.1073/pnas.1118029109>

592 Wickham, H., 2009. *ggplot2: Elegant Graphics for Data Analysis*.

593 Widdel, K., Knittel, A., Galushko, F., 2010. Anaerobic Hydrocarbon- Degrading
594 Microorganisms: An Overview, in: Timmis, N.K., McGenity, T., Meer, J.R., Lorenzo, V.
595 (Eds.), *Handbook of Hydrocarbon and Lipid Microbiology*. pp. 1997–2022.
596 <https://doi.org/10.1007/978-3-540-77587-4>

597 Wood, S., 2011. Mixed GAM Computation Vehicle with GCV/AIC/REML smoothness
598 estimation and GAMMs by REML/PQL.

599 Wood, S., 2006. Low rank scale invariant tensor product smooths for generalized additive
600 mixed models. *Biometrics* 62, 1025–1036.

601 Woulds, C., Bouillon, S., Cowie, G.L., Drake, E., Middelburg, J.J., Witte, U., 2016. Patterns
602 of carbon processing at the seafloor: The role of faunal and microbial communities in
603 moderating carbon flows. *Biogeosciences* 13, 4343–4357. <https://doi.org/10.5194/bg-13->

604 4343-2016

605 Zetsche, E., Paterson, D.M., Lumsdon, D.G., Witte, U., 2011. Temporal variation in the
606 sediment permeability of an intertidal sandflat. *Mar. Ecol. Prog. Ser.* 441, 49–63.
607 <https://doi.org/10.3354/meps09390>

608 Zhao, X., Gong, Y., O'Reilly, S.E., Zhao, D., 2015. Effects of oil dispersant on solubilization,
609 sorption and desorption of polycyclic aromatic hydrocarbons in sediment–seawater
610 systems. *Mar. Pollut. Bull.* 92, 160–169. <https://doi.org/10.1016/j.marpolbul.2014.12.042>

611 Zuidgeest, A., Huettel, M., 2012. Dispersants as Used in Response to the MC252-Spill Lead
612 to Higher Mobility of Polycyclic Aromatic Hydrocarbons in Oil-Contaminated Gulf of
613 Mexico Sand. *PLoS One* 7, e50549. <https://doi.org/10.1371/journal.pone.0050549>

614